Sottrup-Jensen, L., Stepanik, T. M., Jones, C. M., Lønblad, P. B., Kristensen, T., & Wierzbicki, D. M. (1984b) *J. Biol. Chem. 259*, 8293–8303.
Sottrup-Jensen, L., Gliemann, J., & Van Leuven, F. (1986) *FEBS Lett. 205*, 20–24.
Swenson, R. P., & Howard, J. B. (1979) *J. Biol. Chem. 254*, 4452–4456.
Tabor, S., & Richardson, C. C. (1987) *Proc. Natl. Acad. Sci. U.S.A. 84*, 4767–4771.
Tack, B. F., Harrison, R. A., Janatova, J., Thomas, M. L., & Prahl, J. W. (1980) *Proc. Natl. Acad. Sci. U.S.A. 77*, 5764–5768.
Thim, L., Bjoern, S., Christensen, M., Nicholaisen, E. M., Lund-Hansen, T., Pedersen, A. H., & Hedner, U. (1988) *Biochemistry 27*, 7785–7793.
Van Leuven, F., Cassiman, J.-J., & Van den Berghe, H. (1979) *J. Biol. Chem. 254*, 5155–5160.
Van Leuven, F., Cassiman, J.-J., & Van den Berghe, H. (1981) *J. Biol. Chem. 256*, 9016–9022.
Van Leuven, F., Marynen, P., Sottrup-Jensen, L., Cassiman, J.-J., & Berghe, H. (1986) *J. Biol. Chem. 261*, 11369–11373.
Waechter, D. E., & Baserga, R. (1982) *Proc. Natl. Acad. Sci. U.S.A. 79*, 1106–1110.
Wang, D., Wu, K., & Feinman, R. D. (1981) *Arch. Biochem. Biophys. 211*, 500–506.
Wang, D., Yuan, A. I., & Feinman, R. D. (1983) *Ann. N.Y. Acad. Sci. 421*, 90–97.

Ligand-Induced Myosin Subfragment 1 Global Conformational Change†

Stefan Highsmith* and Don Eden

Department of Biochemistry, University of the Pacific, School of Dentistry, San Francisco, California 94115, and Department of Chemistry and Biochemistry, San Francisco State University, San Francisco, California 94132

Received August 25, 1989; Revised Manuscript Received November 20, 1989

ABSTRACT: The effects of selected ligands on the structure of myosin subfragment 1 (S1) were compared by using transient electrical birefringence techniques. With pairs of dilute solutions of S1 at 3.5 °C in low ionic strength (μ = 0.020 M) buffers that had matched electrical impedances, S1 with Mg^{2+}, MgADP, or MgADP·V_i bound was subjected to 6–7-μs external electrical fields in the Kerr law range. Specific Kerr constants and the rates of rotational Brownian motion after the electric field was removed were measured. Neither Mg^{2+} nor MgADP had a measurable effect on either observable, but when orthovanadate (V_i) bound S1·MgADP it decreased the rotational correlation coefficient from 267 ± 6 to 244 ± 10 ns. Parallel measurements of MgATPase activity indicated that S1·MgADP·V_i was greater than 95% inhibited. These results confirm the conclusion of Aguirre et al. [(1989) *Biochemistry 28*, 799] that V_i binding to S1·MgADP increases its rate of rotational Brownian motion and provide data that are more quantitatively correlated with S1 structure. The V_i-induced change in the rotational correlation coefficient is consistent with S1 becoming more flexible or more compact when V_i binds. Assuming that S1·MgADP·V_i is an analogue for S1·MgADP·P_i, the structural changes observed for S1–ligand complexes in solution are discussed in relation to possible structural changes of intermediates on the kinetic pathway of ATPase hydrolysis. A new model of force generation by S1 in muscle is hypothesized.

The nature of the adenosine 5′-triphosphate (ATP)[1]-driven structural change of the actomyosin complex, which generates force in muscle, is unknown. The binding to and hydrolysis of MgATP by actomyosin comprise the chemical event hypothesized to explain the increase in muscle tension that occurs with increasing overlap of the thick and thin filaments (Huxley & Hanson, 1954; Huxley & Niedergerke, 1954). In solutions that approximate intracellular conditions, the kinetic pathway involves a cycle of myosin binding to and dissociating from actin for each MgATP hydrolyzed (Lymn & Taylor, 1971; Eisenberg & Kielley, 1973; Inoue & Tonomura, 1974). Force to slide filaments by one another in muscle is generated, presumably in an analogous cycle, by a myosin structural change between two bound states (Huxley, 1969; Huxley & Simmons, 1971; Nehei et al., 1974). This structural change is thought to be accompanied by an increase in the stability of the actomyosin complex and is usually characterized as some combination of the subfragment 1 (S1) portion of myosin rolling on actin, and/or S1 bending while bound, and/or actin rolling to rotate bound S1. Spectroscopically detected changes have been reported in the orientation of some but not all of the orientation-sensitive probes that have been attached to the S1 portion of myosin in fibers (Borejdo et al., 1979, 1982; Thomas & Cooke, 1980; Yanagida, 1981; Ajtai & Burghardt,

†Supported by NIH Grants AR37499 and GM31674 to S.H. and D.E., respectively.

*Address correspondence to this author at the Department of Biochemistry, University of the Pacific, School of Dentistry.

[1] Abbreviations: M, myosin; S1, myosin subfragment 1; TEB, transient electric birefringence; Δn, birefringence; τ_L, rotational correlation coefficient (=$1/6\theta$, where θ is the rotational diffusion coefficient) obtained from the decay of the birefringence from a steady-state signal; K_{sp}, specific Kerr constant; K_a, association constant; χ_B, angular displacement of one segment of a rigid cylinder bent at the center; Δd, linear displacement of the tip of one segment of a rigid bent cylinder away from the axis of the other segment; V_i, orthovanadate; P_i, orthophosphate; N, nucleotide; ATP, adenosine 5′-triphosphate; ADP, adenosine 5′-diphosphate; EDTA, ethylenediaminetetraacetate; SDS, sodium dodecyl sulfate.

0006-2960/90/0429-4087$02.50/0

1987; Svensson & Thomas, 1988). These changes in probe orientation are consistent with the idea that S1, or part of it, changes orientation during the interaction of myosin with MgATP and actin.

A major goal is to correlate S1 structural changes with intermediates on the kinetic pathway of MgATP hydrolysis. One of the routes to this goal is the study of myosin and its proteolytic fragments in solution, using purified proteins and well-defined conditions. During MgATP hydrolysis by myosin (M) in solution at pH 8, the major steady-state intermediate is M**·MgADP·P (Trentham et al., 1972; Bagshaw & Trentham, 1974). The M** refers to myosin-enhanced tryptophan absorbance and fluorescence during steady-state hydrolysis (Morita, 1967; Werber et al., 1972). The fraction of total bound myosin that is the intermediate M** in kinetic analyses changes with temperature (Bagshaw & Trentham, 1974), and temperature-dependent S1-localized conformational changes also have been detected directly (Shriver & Sykes, 1981a,b; Shriver, 1984). The species M**·MgADP·P is a candidate for the weakly bound actin-bound intermediate that exists before the structural change that generates force (Reedy et al., 1965; Taylor, 1979; Eisenberg & Greene, 1980). This intermediate is too labile to be isolated, but a stable analogue has been synthesized by Goodno (1979, 1982; Goodno & Taylor, 1982), who replaced P_i with the analogue vanadate (V_i). The analogue M·MgADP·V is not identical with M**·MgADP·P, but it has several structural similarities (Wells & Bagshaw, 1984; Goodno & Taylor, 1982). If the global structure of M·MgADP·V is significantly different from the structures of other intermediates on the kinetic pathway of ATP hydrolysis, then the difference should be considered as possibly due to a force-generating structural change that myosin makes while bound to actin.

Such a structural difference has been reported by Aguirre et al. (1989), who observed a 31% increase in the rate of S1 rotational Brownian motion in solution, as determined from the polarized emission from a bound fluorescent ADP analogue, when V_i was also bound to the complex. The absolute values for the rates of rotational Brownian motion were too small to be consistent with the known dimensions of S1 rotating about a minor axis. However, if the probe is accurately reporting changes in the rotational motion of the protein, this increase in rotational rate suggests that S1·MgADP·V may be substantially more compact than S1·MgADP (Aguirre et al., 1989).

In the present study, the rotational dynamics of S1 in the presence of several ligands were investigated by the technique of transient electrical birefringence (TEB). In use of this very sensitive technique that does not require an extrinsic probe, a uniform electric field is briefly applied to a solution of S1. While the field is present, the torque created by the interaction of the applied field and the large permanent dipole moment of S1 tends to align the molecule with the field. If the field is on long enough, a steady-state degree of alignment is obtained, which depends on the strength of the applied field, the size of the electric dipole moment, and the temperature of the solution. The alignment of S1 makes the solution birefringent. When the field is removed, the S1 alignment is randomized by rotational Brownian motion, and the birefringence signal decays. TEB has been used to measure S1 electric dipole moment and hydrodynamic properties (Highsmith & Eden, 1986, 1987). In the current study, the binding of V_i to S1·MgADP is shown to decrease the size of the steady-state birefringence signal for a given field strength and to increase the rate of decay of the signal. The absolute values of the rotational correlation coefficients obtained by using TEB are more quantitatively consistent with S1 structure, and the increase in the rate of rotational Brownian motion is smaller than reported by Aguirre et al. (1989). The differences in the results obtained by the two techniques are discussed along with possible assignments of S1 conformational changes to intermediates on the kinetic pathway of ATP hydrolysis.

Materials and Methods

Proteins and Chemicals. Myosin was isolated from New Zealand albino rabbit dorsal muscle according to Nauss et al. (1969) and used for the α-chymotryptic preparation of S1 in the absence of Mg^{2+} (Weeds & Taylor, 1976). S1 containing only light chain 1 was isolated by using a DE52 anion-exchange resin eluted with a 0–0.18 M NaCl linear gradient, similar to the procedure of Weeds and Taylor (1976). This S1 was precipitated with 60% ammonium sulfate and then dialyzed exhaustively to remove ammonium sulfate and obtain solutions suitable for TEB measurements. S1 MgATPase activity was typically $0.051 \pm 0.020\ s^{-1}$ when measured at 22 °C, pH 7.0, for steady-state conditions by the method of Imamura et al. (1966). Polyacrylamide gel electrophoresis in the presence of SDS was done as reported previously (Highsmith & Eden, 1985). Chemicals were reagent grade and were used without further purification. Stock 10 mM Na_3VO_4 and Na_3PO_4 solutions were freshly made, boiled, and adjusted to pH 7.0 with HCl.

TEB Sample Preparation. An S1 stock solution was dialyzed at 4 °C against 10 mM Tris–acetate (Trisma base plus glacial acetic acid to attain pH 7.0 at 4 °C), 0.40 mM $MgCl_2$, and 0.050 mM EDTA. After four to six changes of 1000:1 (v/v) dialysis buffer, the sample was centrifuged at 80000*g* for 1 h and then diluted to 3–15 μM S1 with the same buffer. ADP in the same buffer was added in a small volume to obtain more than 0.30 mM ADP. The sample was divided into two equal portions, and identical volumes of Na_3VO_4 or Na_3PO_4 plus buffer were added to obtain 0.30 mM vanadate or phosphate, respectively, and 0.30 mM ADP. The final [S1] was typically 2–3 μM. Phosphate does not bind S1·MgADP under these conditions. This procedure produces S1·MgADP·V and S1·MgADP in solutions that have nearly identical electrical impedances, typically in the 330–400 Ω range as measured in the birefringence cell at 3.7 °C, depending on the actual electrolyte concentrations. A given pair of samples had impedances that differed by less than 5%. Solutions of S1 used to compare the effects of $MgCl_2$ vs MgP_i and MgP_i vs MgADP were prepared similarly to those for MgADP·V vs MgADP in order to obtain matched pairs.

Instruments and Measurements. The transient electric birefringence experiments were performed with an apparatus similar to that described previously (Highsmith & Eden, 1985, 1986, 1987). A reference cell filled with water was placed in the optical path and exposed to the simultaneous electric field of equal strength and perpendicular orientation in order to compensate for the birefringence of the solvent. The high-voltage pulses were provided by a Velonex Model 360 pulse generator. The terminated output of the photomultiplier tube was amplified by a factor between 20 and 400, depending on the applied field strength, using a Comlinear E103 in series with one stage of a LeCroy 6103 amplifier. The overall bandwidth was DC–125 MHz. The signal was then sent to a LeCroy 100-MHz transient digitizer in a LeCroy 8013 CAMAC crate. The data were transferred to an IBM AT compatible computer via an IEEE488 interface. The number of pulses averaged was a function of the applied electric field and ranged from 100 to 4000. The applied electric field was

measured by using a Phillips 8931 100:1 high-voltage probe and a LeCroy 6103 amplifier used with a gain of 0.01, followed by the LeCroy 100-MHz digitizer.

Data Analysis. The digitized transient electric birefringence signal was processed by first subtracting a signal that can be ascribed to electronic pickup. The pickup signal is obtained by collecting data in the usual way except for having the laser beam blocked from reaching the photomultiplier tube. Conversion of the intensity variation to birefringence is carried out in a standard manner (Eden & Elias, 1983). The average value of the birefringence for the last 350 ns of the steady-state signal with the field applied was used in the determination of the Kerr constants (Highsmith & Eden, 1985). The birefringence decay was analyzed to determine rotational diffusion constants using Provencher's (1976a, 1976b) program DISCRETE. Decay analyses that started with the first few channels after the field was removed resulted in rotational times that were longer than those that began with later channels. This result is not expected. Starting the decay analysis at a later time resulted in an increase in the signal-to-noise ratio. We believe that this behavior was due to a small but significant jitter in the pulse width of the high-voltage pulse generator. The source of the effect was not detected until after the experiments were completed. Therefore, we have analyzed our decay curves beginning at times that are significantly (up to 100 ns) after the end of the excitation pulse to avoid this complication. Initiation of the analysis at this time precludes our resolution of decay processes that may exist but have decayed before the time at which we begin analysis. The procedure used here also may be the reason that the rotational correlation coefficients [$\tau_L = (6\theta)^{-1}$, where θ is the rotational diffusion coefficient] for S1 are somewhat smaller than previously reported (Highsmith & Eden, 1987).

RESULTS

S1·MgADP·V Complex. The effectiveness of orthovanadate as an inhibitor of myosin ATPase activity and the very slow rate of dissociation of V_i from the inhibited M·MgADP·V complex are well established for myosin and S1 in solutions of higher ionic strength and pH than were employed here (Goodno, 1979, 1982; Goodno & Taylor, 1982; Wells & Bagshaw, 1984). The existing range of conditions that promote and stabilize the inhibited S1 complex was expanded to include combinations of lower ionic strength, neutral pH, and lower [V_i] and [ADP], which were used in subsequent experiments for technical reasons.

When 96 μM S1 was incubated at 25 °C in 25 mM KCl, 1 mM $MgCl_2$, 10 mM MOPS (pH 7.0), 0.27 mM ADP, and 0.60 mM Na_3VO_4 and aliquots were taken over time and analyzed for MgATPase activity, over 95% of the activity was lost within 30 min (Figure 1A). If after 30-min incubation the inhibited S1 was diluted so that the final total conditions were 0.61 μM S1, 0.250 mM KCl, 1 mM $MgCl_2$, 10 mM MOPS (pH 7.0), 0.027 mM ADP, and 0.060 mM Na_3VO_4 at 0 °C, activity was regained slowly, over several hours (Figure 1B).

The loss of MgATPase activity due to vanadate binding for aliquots of S1 assayed as described above was used to estimate the amount of S1·MgADP·V formed in the solutions used for TEB measurements. For 1–5 μM S1, 0.30 mM ADP, 0.30 mM Na_3VO_4, 0.40 mM $MgCl_2$, and 0.050 mM EDTA at pH 7.0 incubated at 4 °C in 10 mM Tris–acetate, the equilibrium constant

$$K = [S1\cdot MgADP\cdot V]/[S1][MgADP][V_i]$$

for complex formation was estimated to be greater than 3×10^8 M^{-2}. This value is consistent with the equilibrium constant of about 10^9 M^{-2} observed at higher pH, ionic strength, and temperature (Goodno, 1979; Goodno & Taylor, 1982). The inhibition of S1 MgATPase was not reduced significantly by the TEB measurements, when assayed at 25 °C after the measurements were completed, suggesting that the applied electric field is benign. One exception was a sample in which the $MgCl_2$ concentration was 4.0 mM instead of 0.40 mM during the TEB measurements. In that case, for reasons that are not clear, the after-experiment activity of the S1 was 16% of that of control S1, rather than the 3–8% typically observed.

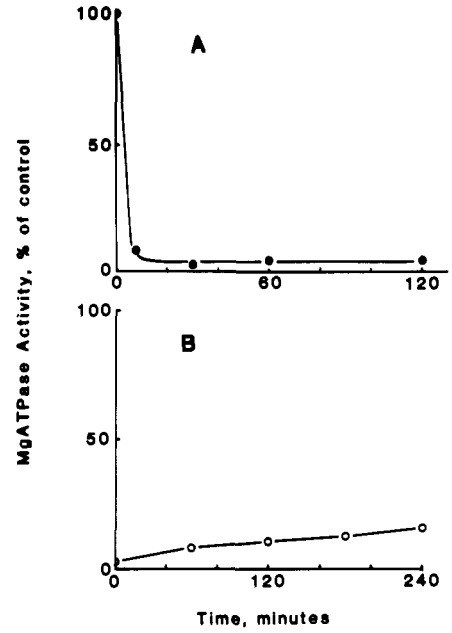

FIGURE 1: Formation and stability of S1·MgADP·V. (A) The loss of S1 MgATPase activity as percent of control was determined for increasing time of incubation in 25 mM KCl, 1 mM $MgCl_2$, 10 mM MOPS (pH 7.0, KOH), 0.27 mM ADP, and 0.60 mM Na_3VO_4 at 25 °C by taking aliquots and analyzing ADP production by the method of Imamura et al. (1966). (B) The reversal of MgATPase inhibition was determined for increasing lengths of time after diluting 97%-inhibited S1 solutions described under (A) to 0.61 μM S1, 0.250 mM KCl, 10 mM MOPS (pH 7.0), 1 mM $MgCl_2$, 0.027 mM ADP, and 0.060 mM Na_3VO_4 at 0 °C.

The S1·MgADP·V samples were not exposed to intense irradiation in the 300–400-nm range that might cause ATP site modification or S1 heavy-chain cleavage (Cremo et al., 1988; Grammer et al., 1988; Mocz, 1989), nor were large or small cleavage products detected on SDS–polyacrylamide gel electrophoretograms. Small fragments are more difficult to detect by SDS–PAGE, but they would not contribute significantly to the birefringence signal because of their very small K_{sp} and τ values. In conclusion, for the samples used for TEB measurements, the S1·MgADP·V complex is the major species when V_i is present, and the complex does not seem to be destabilized by the measurements.

Field-Free Decay Rates. Solutions of S1 were exposed to electric fields of varying strengths for from 6 to 7 μs, during which time a steady-state birefringence signal is obtained (Highsmith & Eden, 1986). Typical traces of the applied electric field and the resulting birefringence increase (Δn) and decay are shown in panels A and B, respectively, of Figure 2 for 2.6 μM S1 in 10 mM Tris–acetate (pH 7.0 at 4 °C), 0.050 mM EDTA, 0.40 mM $MgCl_2$, 0.30 mM ADP, and 0.30 mM V_i at 3.5 °C. The decay of the signal beyond the region of pulse jitter (see Materials and Methods) was best fit to a single-exponential decay (Provencher, 1976a,b) for solutions of S1 after exposure to applied electric fields between 1070

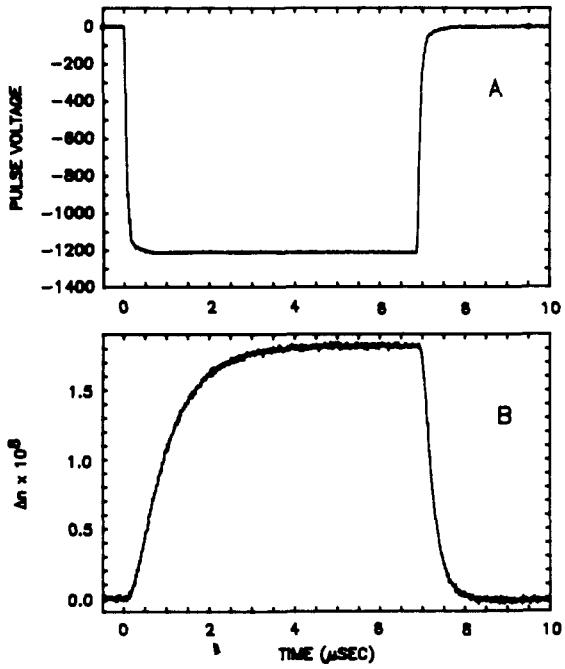

FIGURE 2: Applied electric field and resulting birefringence signal. (A) The trace shows a 1200-V 6.8-μs electric field which was applied across a 0.285-cm sample of 2.3 μM S1·MgADP·V in 10 mM Tris–acetate (pH 7.0 at 4 °C), 0.30 mM $MgCl_2$, and 0.30 mM ADP. Data were collected at 10-ns intervals during the 500 repetitions of the applied field. (B) The trace shows the birefringence signal obtained. The much slower rise compared to the decay is expected for a molecule orienting in the field via a permanent dipole moment.

Table 1: Properties of S1·MgADP·V and S1·MgADP Modeled as Rigid Bent and Straight Cylinders, Respectively

property	S1·MgADP·V	S1·MgADP
K_{sp}	(2.69 ± 0.20) × 10^{-7}	(2.85 ± 0.10) × 10^{-7}
τ_L (ns)	244 ± 10	267 ± 6
χ_B[a]	32	0
Δd[b] (nm)	5.2	0
K_a[c] (M^{-1})	1.5 × 10^3	2.3 × 10^6

[a] The theory of Garcia de la Torre and Bloomfield (1982) was used to model S1 as a rigid straight cylinder for the longer TEB-determined τ_L and as a rigid bend cylinder for the smaller τ_L. Placing the bend point at the center, χ_B is the angular displacement one segment must make to reduce τ_L by 9%. τ_L values are for 3.5 °C. [b] If the staight cylinder is 19 nm long, then Δd is the distance the end of the cylinder moves frm its original position for a central bend point and χ_B = 32°. [c] Association constants for S1·MgADP (Highsmith, 1976) and S1·MgADP·V (Goodno & Taylor, 1982) binding to F-actin, adjusted to 25 °C and 0.02 M ionic strength.

and 8030 V/cm. This was the case for all the ligands used. No dependence of the rotational correlation coefficient, τ_L, on field strength was observed. Results for S1·MgADP and S1·MgADP·V are shown in Figure 3. The independence of the rate of birefringence decay from a steady-state signal on the field strength confirms earlier observations made on S1 without ligands (Highsmith & Eden, 1986). The average values for the decay constants at 3.5 °C are 267 ± 6 ns (n = 12) and 244 ± 10 ns (n = 12) for S1·MgADP and S1·ADP·V, respectively (see Table I). The 9% decrease in τ_L for S1·MgADP in the presence of V_i is consistent with S1·MgADP being made more compact or more flexible by V_i binding. When the rates of electric field free rotational Brownian motion were measured for S1 in the presence of the ligand pairs Mg^{2+} vs Mg^{2+} plus P_i and Mg^{2+} vs Mg^{2+} plus ADP, no significant or reproducible differences in τ_L values were detected.

Specific Kerr Constants. The average steady-state birefringence (Δn) increased linearly with the square of the applied

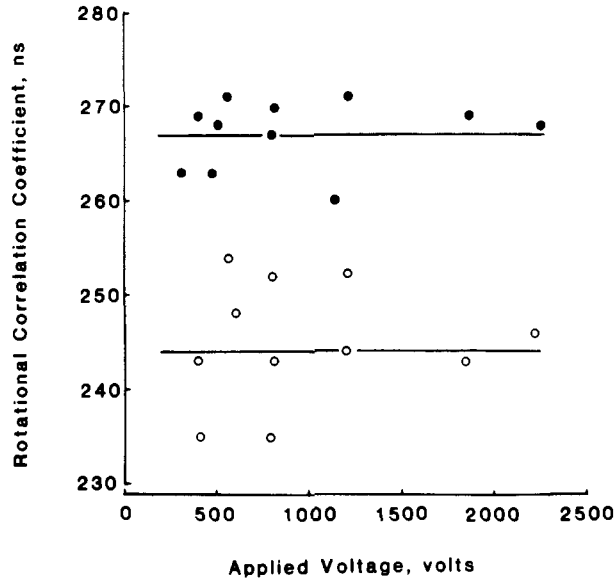

FIGURE 3: Field-free rotational Brownian motion of S1·MgADP and S1·MgADP·V. The rotational correlation coefficient, τ_L, was determined at 3.5 °C as described in the text for S1·MgADP (●) and S1·MgADP·V (○) for decay after removing applied voltages between 0 and 2000 V or fields between 0 and 23.4 statvolts/cm. Data are from the three S1 preparations. The uncertainty for each measurement of τ_L is ±3%. The average τ_L values are 267 ± 6 and 244 ± 10 ns for S1·MgADP and S1·MgADP·V, respectively.

electric field for paired samples of S1 and field strengths from 1400 to 8700 V/cm. Specific Kerr constants, K_{sp}, were calculated by using the expression $K_{sp} = \Delta n/C_v 1.33E^2$ where C_v is the volume fraction of S1 and E is the electric field in statvolts per centimeter. Linear fits to the data (not shown) had correlation coefficients (r) better than 0.999. The specific Kerr constants for S1·MgADP·V and S1·MgADP were (2.69 ± 0.20) × 10^{-7} and (2.85 ± 0.10) × 10^{-7} cm^2/statvolt^2, respectively, when averaged for three S1 preparations in which [S1] was between 2 and 14 μM (see Table I). These values are near that obtained by using this range of electric fields for S1 in the absence of nucleotide (Highsmith & Eden, 1985). The apparent 5% decrease in K_{sp} for S1·MgADP·V, compared to that for S1·MgADP, is not statistically significant when judged by the F test (Snedecor & Cochran, 1967). Parallel measurements on matched paired solutions of S1 in the presence of Mg^{2+} vs Mg^{2+} plus P_i and Mg^{2+} vs Mg^{2+} plus ADP did not indicate any apparent differences in their specific Kerr constants.

Discussion

The 9% decrease in the rotational relaxation time when V_i is bound to S1·MgADP may be due to increased S1 segmental flexibility or to a reduction of its longest dimension. When S1·MgADP·V is used as an analogue of S1·MgADP·P during ATP hydrolysis, the structural change observed here for S1 corresponds to the step S1·MgADP·P → S1·MgADP + P_i, which for S1 bound to actin is a candidate for the force-producing step (Taylor, 1979; Webb et al., 1986). Isolated S1 in solution appears to get longer and/or less flexible for the corresponding reaction.

First consider interpreting the change in τ_L using a model of increasing S1 segmental flexibility. Changes in the segmental flexibility of S1 have been observed (Highsmith & Eden, 1986, 1987). More localized indications of S1 flexibility have also been inferred from results from S1 cross-linking experiments (Burke & Reisler, 1977; Wells & Yount, 1979; Lu et al., 1986; Huston et al., 1988), fluorescence energy

transfer (Dalbey et al., 1983), and bound nucleotide behavior (Perkins et al., 1984; Cheung et al., 1985; Shriver & Sykes, 1981a; Aguirre et al., 1986). A model of changing S1 flexibility is not easily correlated to specific mechanical events like rolling or bending. However, a decrease in segmental flexibility for the S1·MgADP·V to S1·MgADP step, if that is the correct interpretation of our data, is consistent with the NMR-detected loss of side-chain and backbone flexibility (Highsmith et al., 1979; Highsmith & Jardetzky, 1980; Prince et al., 1981; Eads & Mandelkern, 1984) and the reduced proteolytic susceptibility (Doung & Reisler, 1989) which occurs when S1 goes from unbound (or weakly bound) to rigor in the presence of actin. The idea that S1 would be structurally more rigid after it generated force than it was before is reasonable and perhaps required a priori. If bound S1 is acting as a leverlike projection to generate and maintain force, it is *not* reasonable that it would have become more segmentally flexible at the end of the process.

An alternative interpretation of the results can be made by using a segmented model of S1 that can assume two rigid conformations, one (S1·MgADP·V) more compact than the other (S1·MgADP). With this approach, it is possible to quantitatively correlate ligand-induced changes in S1 structure in solution to crossbridge mechanics in muscle fibers. There is evidence that S1 undergoes segmental motion. S1 free of nucleotides in solution behaves like a flexibly segmented molecule (Highsmith & Eden, 1986, 1987). Nucleotide binding to S1 increases the distance from the 633–642 region to Cys-697 but not to Cys-707 as monitored by fluorescence energy transfer (Kasprzak et al., 1989; Botts et al., 1989), which is consistent with segmental motion. Electron micrographs of negatively stained myosin show S1 portions that appear to be segmented and to be in either straight or bent configurations (Walker & Trinick, 1988). When bound to actin, S1·MgADP·V appears to be smaller and rounder than S1·MgADP (Katayama, 1989). The 9% change in the rotational correlation (Table I) coefficient corresponds to a 3% change in S1's longest dimension when it is modeled as a rigid cylinder that is either straight or bent at its center (Garcia de la Torre & Bloomfield, 1982). Choosing a two-state model and placing the bend point at the center are arbitrary. This modest change in length is coupled to a substantial degree of bending or straightening. S1 is about 19 nm long (Elliott & Offer, 1978; Highsmith & Eden, 1986, 1987; Walker & Trinick, 1989). If a straight 19-nm rod is bent at its midpoint so that half of it rotates away from the long axis in order to make the end-to-end distance 3% smaller, the rotation is 32°, and the displacement of one end of the rod from its position on the original axis is 5.2 nm (see Table I and Figure 4A). If this rod were imbedded in S1, one end of S1 would move 5.2 nm during the transition from S·MgADP·V to S1·MgADP as S1 went from bent to straight. Adding a nonhydrolyzable ATP analogue to muscle fibers has been shown to increase the half-sarcomere length by 2 nm (Marston et al., 1979). Huxley and Kress (1985) have reviewed the results from a variety of measurements and suggested that the complete crossbridge force-generating displacement in muscle may be as small as 4 nm.

It is possible to correlate this S1 straightening interpretation of the V_i-induced change in S1 rotational hydrodynamics to the known changes in S1 affinity for actin (see Table I). S1, nucleotide (N), and actin form a ternary complex for which the stability is determined by ATP binding subsite occupancy (Highsmith, 1976). The affinity of S1·N for actin increases at least 10^4-fold in several steps as MgATP is hydrolyzed and

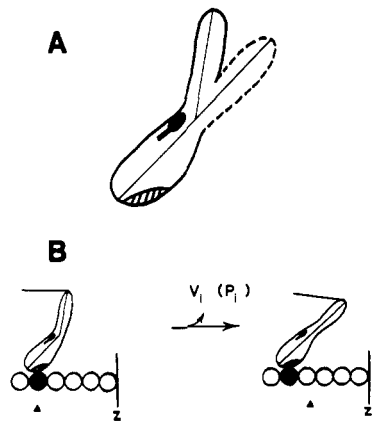

FIGURE 4: Modeling S1 structural changes. The change in S1 hydrodynamic mobility which is induced by V_i binding to S1·MgADP is consistent with a transition from a rigid linear to a rigid bent S1, using the theory of Garcia de la Torre and Bloomfield (1982; see text and Table I). (A) Isolated S1·MgADP·V and S1·MgADP are shown in a composite diagram. The all-solid outline of a bent S1 represents S1·MgADP·V. The half-solid and half-dashed outline represents S1·MgADP. The segment moves through 32°, and its tip traverses 5.2 nm if the length of S1 is 19 nm. The solid keyhole-shaped symbol represents the ATP binding site, and the hatched area represents the actin binding site, located on S1 as indicated by the results of Tokunaga et al. (1987). (B) The hypothesized structural change S1 undergoes in solution as the occupancy of the ATP binding site changes from MgADP·V to MgADP is shown for S1 bound to actin in a muscle fiber. In this speculative model of force generation, S1 straightening moves the actin to which it is bound by about 5.2 nm (the triangle provides a fixed position). MgADP·V is an analogue of MgADP·P, and the step shown in (B) corresponds to the phosphate release step. The thin filament is represented by a row of circles, the connection to the thick filament by a line from the top of S1, and the Z disk by a vertical line.

dissociated (Highsmith, 1976; Greene & Eisenberg, 1978). Similarly, the affinity of S1·MgADP for actin is about 10^3-fold greater than is that of S1·MgADP·V (Goodno & Taylor, 1982). The species S1·MgATP or S1·MgADP·P are believed to bind to actin before the force-generating step occurs (Reedy et al., 1965; Eisenberg & Greene, 1980). The results in Table I suggest that the known increase in actin affinity and the hypothesized S1 straightening are correlated for the S1·MgADP·P → S1·MgADP transition, assuming that MgADP·V is a suitable analogue of MgADP·P. This would allow the free energy decrease obtained from stronger actomyosin binding to be used for force production. In this hypothesis, a bent S1·MgADP·P would bind actin and then straighten to move actin 5.2 nm as P_i is released and actin affinity increases (Figure 4B).

When the rotational correlation coefficients obtained at 10 °C from anisotropy measurements of ϵADP bound to S1 (Aguirre et al., 1989) and those obtained at 3.5 °C from TEB (Table I) are adjusted to 20 °C values, one obtains τ_{fl} equal to 79 and 55 ns and τ_L equal to 159 and 145 ns for the $-V_i$ and $+V_i$ cases, respectively. The τ_{fl} values are much smaller than the τ_L values, and the V_i-induced decrease in τ_{fl} is 31% rather than the 9% reported here. The τ_{fl} values are in good agreement with rotational correlation coefficients obtained from ATP site bound fluorescent (Perkins et al., 1984; Cheung et al., 1985; Aguirre et al., 1986) and NMR (Shriver & Sykes, 1981b) probes. Rotational correlation coefficients obtained from the anisotropy of fluorescent probes located away from the ATP site (Mendelson et al., 1973) are much closer to the τ_L values obtained by using TEB. It has been suggested that the ATP site is itself flexible (Perkins et al., 1984).

It was possible to simulate fluorescence anisotropy [$A(t)$] decay data by using a linear combination of the observed TEB

τ_L and a shorter τ_S (assigned to local motion of the ATP site or probe), which when fit to a single-exponential decay function gave a calculated best fit with τ_{calcd} equal to τ_{fl}. Specifically, $A(t)$ values generated by using $A(t) = A(0)[(1 - f_s) \times \exp(-t/159\text{ ns}) + f_S \exp(-t/\tau_S)]$ were consistent with $\tau_{calcd} = 79$ ns when fit to the equation $A(t) = A(0) \exp(-t/\tau_{calcd})$ for a set of paired values of f_S and τ_S. Thus, the observed rotational correlation coefficients obtained in the absence of V_i from ϵADP fluorescence anisotropy decay ($\tau_{fl} = 79$ ns) and field-free birefringence decay ($\tau_L = 159$ ns) can be shown to be consistent with each other by adding an internal mode of fluorescence depolarization (τ_S) to the end-over-end rotation of S1 (τ_L). However, using this simple approach, it was not possible to simulate data that were fit by a 31% smaller τ_{calcd} when τ_L was changed from 159 to 145 ns, without also changing f_S and τ_S. If τ_L was decreased and f_S and τ_S were held constant, the largest decrease in τ_{calcd} was 8%. This unsuccessful attempt to reconcile the V_i-induced changes in τ_L and τ_{fl} while keeping the contribution from the ATP site internal motion constant suggests that V_i binding increases the local mobility of ϵADP or changes the alignment of its fluorescence emission dipole relative to the long axis of S1. It is possible that binding V_i would change the average orientation of the adenine moiety of ϵADP. On the other hand, nucleotides and V_i binding are known to increase the local flexibility of S1 at other sites (Seidel & Gergely, 1973; Wells & Bagshaw, 1984), and V_i binding may increase flexibility at the ATP site as well.

However, inspite of any quantitative problems with measuring S1 rotation using ATP site probes, the TEB results presented here confirm the Aguirre et al. (1989) report that the apparent rate of rotational Brownian motion of S1·MgADP is increased by V_i binding. This change in S1-equivalent hydrodynamic structure, which is caused by changes in ligand occupancy of the ATP binding site and correlated with changes in actin affinity, is consistent with ligand-induced S1 force generated by a bent to straight conformational change. This is the first quantitative correlation of a modeled nucleotide-induced S1 structural change in solution to the mechanical requirements of force production in muscle.

ACKNOWLEDGMENTS

We thank Mary Ling and Howard Higson for technical assistance and Barbara Chacon-Esquibel for preparing the manuscript.

REFERENCES

Aguirre, R., Gonsoulin, F., & Cheung, H. C. (1986) *Biochemistry 25*, 6825–6835.
Aguirre, R., Lin, S.-H., Gonsoulin, F., Wang, C.-K., & Cheung, H. C. (1989) *Biochemistry 28*, 799–807.
Ajtai, K., & Burghardt, T. P. (1987) *Biochemistry 26*, 4517–4523.
Bagshaw, C., & Trentham, D. R. (1974) *Biochem. J. 141*, 331–349.
Borejdo, J., Putnam, S., & Morales, M. F. (1979) *Proc. Natl. Acad. Sci. U.S.A. 76*, 6346–6350.
Borejdo, J., Assulin, O., Ando, T., & Putnam, S. (1982) *J. Mol. Biol. 158*, 391–414.
Botts, J., Thomaseon, J. F., & Morales, M. F. (1989) *Proc. Natl. Acad Sci. U.S.A. 86*, 2204–2208.
Burke, M., & Reisler, E. (1977) *Biochemistry 16*, 5559–5563.
Cheung, H. C., Gonsoulin, F., & Garland, F. (1985) *Biochim. Biophys. Acta 832*, 52–62.
Cremo, C. R., Grammer, J. C., & Yount, R. G. (1988) *Biochemistry 27*, 8408–8415.
Dalbey, R. E., Weiel, J., & Yount, R. G. (1983) *Biochemistry 22*, 4696–4706.
Doung, A. M., & Reisler, E. (1989) *Biochemistry 28*, 3502–3509.
Eads, T., & Mandelkern, L. (1984) *J. Biol. Chem. 259*, 10689–10694.
Eden, D., & Elias, J. G. (1983) in *Measurement of Suspended Particles by Quasi-elastic Light Scattering* (Dahneke, B., Ed.) Wiley, New York.
Eisenberg, E., & Kielley, W. W. (1973) *Cold Spring Harbor Symp. Quant. Biol. 37*, 145–152.
Eisenberg, E., & Greene, L. E. (1980) *Annu. Rev. Physiol. 42*, 293–309.
Elliott, A., & Offer, G. (1978) *J. Mol. Biol. 123*, 505–519.
Garcia, de la Torre, J., & Bloomfield, V. (1982) *Q. Rev. Biophys. 14*, 81–139.
Goodno, C. C. (1979) *Proc. Natl. Acad. Sci. U.S.A. 76*, 2620–2624.
Goodno, C. C. (1982) *Methods Enzymol. 85*, 116–123.
Goodno, C. C., & Taylor, E. W. (1982) *Proc. Natl. Acad. Sci. U.S.A. 79*, 21–25.
Goody, R. S., & Holmes, K. C. (1983) *Biochim. Biophys. Acta 726*, 13–39.
Grammer, J. C., Cremo, C. R., & Yount, R. G. (1988) *Biochemistry 27*, 8408–8415.
Greene, L. E., & Eisenberg, E. (1978) *J. Biol. Chem. 255*, 543–548.
Highsmith, S. (1976) *J. Biol. Chem. 251*, 6170–6172.
Highsmith, S., & Jardetzky, O. (1980) *FEBS Lett. 121*, 55–60.
Highsmith, S., & Eden, D. (1985) *Biochemistry 24*, 4917–4924.
Highsmith, S., & Eden, D. (1986) *Biochemistry 25*, 2237–2244.
Highsmith, S., & Eden, D. (1987) *Biochemistry 26*, 2747–2750.
Highsmith, S., Akasaka, K., Konrad, M., Goody, R., Holmes, K., Wade-Jardetzky, N., & Jardetzky, O. (1979) *Biochemistry 18*, 4238–4244.
Huston, E. E., Grammer, J. C., & Yount, R. G. (1988) *Biochemistry 27*, 8945–8952.
Huxley, A. F., & Neidergerke, R. C. (1954) *Nature 173*, 971–973.
Huxley, A. F., & Simmons, R. M. (1971) *Nature (London) 233*, 533–538.
Huxley, H. E. (1969) *Science (Washington, D.C.) 164*, 1356–1366.
Huxley, H. E., & Hanson, J. (1954) *Nature 173*, 973–976.
Huxley, H. E., & Kress, M. (1985) *J. Muscle Res. Cell Motil. 6*, 153–161.
Imamura, K., Tada, M., & Tonomura, Y. (1966) *J. Biochem. (Tokyo) 59*, 280–289.
Inoue, A., & Tonomura, Y. (1974) *J. Biochem. 76*, 755–764.
Kasprzak, A., Chaussepied, P., & Morales, M. F. (1989) *Biophys. J. 55*, 441A.
Katayama, E. (1989) *J. Biochem. (Tokyo) 106*, 751–770.
Lu, R. C., Moo, L., & Wong, A. G. (1986) *Proc. Natl. Acad. Sci. U.S.A. 83*, 6392–6396.
Lymn, R. W., & Taylor, W. E. (1971) *Biochemistry 10*, 4617–4624.
Marston, S. B., Tregear, R. T., Rodger, C. D., & Clarke, M. L. (1979) *J. Mol. Biol. 128*, 111–126.
Mendelson, R. A., Morales, M. F., & Botts, J. (1973) *Biochemistry 12*, 2250–2255.
Mocz, G. (1989) *Eur. J. Biochem. 179*, 373–378.

Morita, F. (1967) *J. Biol. Chem. 242*, 4501–4506.
Nauss, K., Kitagawa, S., & Gergely, J. (1969) *J. Biol. Chem. 244*, 755–765.
Nehei, T., Mendelson, R. A., & Botts, J. (1974) *Proc. Natl. Acad. Sci. U.S.A. 71*, 274–277.
Perkins, W. J., Wells, J. A., & Yount, R. G. (1984) *Biochemistry 23*, 3994–4002.
Prince, H. P., Trayer, H. R., Henry, G. D., Trayer, I. P., Dalgarno, D. C., Levine, B. A., Cary, P. D., & Turner, C. (1981) *Eur. J. Biochem. 121*, 213–219.
Provencher, S. W. (1976a) *Biophys. J. 16*, 27–41.
Provencher, S. W. (1976b) *J. Chem. Phys. 64*, 2772–2777.
Reedy, M. K., Holmes, K. C., & Tregear, R. T. (1965) *Nature (London) 207*, 1276–1280.
Seidel, J., & Gergely, (1973) *Arch. Biochem. Biophys. 158*, 853–863.
Shriver, J. W. (1984) *Trends Biochem. Sci. 9*, 322–328.
Shriver, J. W., & Sykes, B. D. (1981a) *Biochemistry 20*, 6357–6362.
Shriver, J. W., & Sykes, B. D. (1981b) *Biochemistry 20*, 2004–2012.
Snedecor, G. W., & Cochran, W. G. (1967) in *Statistical Methods*, p 116, Iowa State University Press, Ames, IA.
Svensson, E. C., & Thomas, D. D. (1988) *Biophys. J. 50*, 999–1102.
Taylor, E. W. (1979) *CRC Crit. Rev. Biochem. 6*, 103–164.
Thomas, D. D., & Cooke, R. (1980) *Biophys. J. 32*, 891–906.
Tokunaga, M., Sutoh, K., Toyoshima, C., & Wakabayashi, T. (1987) *Nature (London) 329*, 635–638.
Trentham, D. R., Bardsley, R. G., Eccleston, J. F., & Weeds, A. G. (1972) *Biochem. J. 126*, 635–644.
Walker, M., & Trinick, J. (1988) *J. Muscle Res. Cell Motil. 9*, 359–366.
Webb, M. R., Hibberd, M. G., Goldman, Y. E., & Trentham, D. R. (1986) *J. Biol. Chem. 261*, 15557–15564.
Weeds, A. G., & Taylor, R. S. (1976) *Nature (London) 257*, 54–56.
Wells, J. A., & Yount, R. G. (1979) *Proc. Natl. Acad. Sci. U.S.A. 76*, 4966–4970.
Wells, C., & Bagshaw, C. R. (1984) *J. Muscle Res. Cell Motil. 5*, 97–112.
Werber, M. M., Szent-Gyorgi, A. G., & Fasman, G. (1972) *Biochemistry 11*, 2872–2883.
Yanagida, T. (1981) *J. Mol. Biol. 146*, 539–560.

Kinetic and Molecular Orbital Studies on the Rate of Oxidation of Monosubstituted Phenols and Anilines by Horseradish Peroxidase Compound II†

Junji Sakurada,‡ Reiko Sekiguchi, Koichi Sato, and Toichiro Hosoya*
Faculty of Pharmaceutical Sciences, Chiba University, Chiba 260, Japan
Received June 28, 1989; Revised Manuscript Received December 12, 1989

ABSTRACT: The second-order rate constant (k_4) for the oxidation of a series of aromatic donor molecules (monosubstituted phenols and anilines) by horseradish peroxidase (HRP) compound II was examined with a stopped-flow apparatus. The electronic states of these substrates were calculated by an ab initio molecular orbital method. It was found that in both phenols and anilines log k_4 values correlate well with the highest occupied molecular orbital (HOMO) energy level and the lowest unoccupied molecular orbital (LUMO) energy level, but not with the net charge or frontier electron density on atoms of these molecules. The HOMO and LUMO energy levels of phenols and anilines further showed linear relationships with Hammett's σ values with negative slopes. Similar results were obtained in the oxidation of substrates by HRP compound I, except that the rate of reaction was much higher than in the case of HRP compound II. In addition, the rates of oxidation of phenols by compound I or II were found to be about 1000 times higher than those of anilines with similar HOMO energy levels. On the basis of these results, the mechanism of electron transfer from the substrate to the heme iron of HRP compound II is discussed.

It is well established that horseradish peroxidase (HRP)[1] catalyzed reactions proceed in the consecutive steps (Chance, 1951; George, 1952)

$$E + H_2O_2 \xrightarrow{k_1} ES_I \quad (1)$$

$$ES_I + AH_2 \xrightarrow{k_7} ES_{II} + AH^\bullet \quad (2)$$

$$ES_{II} + AH_2 \xrightarrow{k_4} E + AH^\bullet \quad (3)$$

$$AH^\bullet + AH^\bullet \rightarrow A_2H_2 \text{ (or } A + AH_2) \quad (4)$$

where E, ES_I, and ES_{II} are the native enzyme, compound I, and compound II, respectively, and AH_2 and $AH^\bullet$ are the hydrogen donor (the second substrate) and its free radical, respectively. It was reported that the reactions between compound I and AH_2 and between compound II and AH_2 are of the second order and that the rate constant of reaction 2, k_7, is usually much higher than that of reaction 3, k_4 (Chance, 1951; Dunford & Stillman, 1976). However, little is known about the mechanism of electron transfer from the substrate to compound I and compound II.

It was shown recently that cytochrome *c* peroxidase forms a 1:1 complex with cytochrome *c* and that the hemes of the two proteins may be almost parallel with an edge separation of 16.5 Å, suggesting that the electron transfer takes place through an intricate bridge of interaction, ionic interactions, and hydrogen bonds connecting the two hemes (Poulos &

† This work was supported in part by a Grant-in-Aid for Scientific Research from the Ministry of Education, Science and Culture of Japan.
* Address correspondence to this author at the Laboratory of Biophysical Chemistry, Faculty of Pharmaceutical Sciences, Chiba University, Yayoi-Cho 1-33, Chiba, Chiba 260, Japan.
‡ Present address: Department of Bacteriology, Jikei University School of Medicine, Minato-ku, Tokyo 105, Japan.

[1] Abbreviations: HOMO, highest occupied molecular orbital; HRP, horseradish peroxidase; LUMO, lowest unoccupied molecular orbital.

0006-2960/90/0429-4093$02.50/0